Structural and Electronic Properties of Liquid and Amorphous SiO_2: An *Ab Initio* Molecular Dynamics Study

Johannes Sarnthein,[1,2] Alfredo Pasquarello,[1] and Roberto Car[1,3]

[1]*Institut Romand de Recherche Numérique en Physique des Matériaux (IRRMA), IN-Ecublens, CH-1015 Lausanne, Switzerland*

[2]*Institut für Technische Elektrochemie, Technische Universität Wien, A-1060 Wien, Austria*

[3]*Department of Condensed Matter Physics, University of Geneva, CH-1211 Geneva, Switzerland*

(Received 1 September 1994)

We performed a first-principles molecular dynamics study of liquid SiO_2 at a temperature of 3500 K, followed by a rapid quench to 300 K obtaining a perfectly chemically ordered amorphous network. Structural and electronic properties of our amorphous sample are in good agreement with neutron diffraction, x-ray photoemission, and optical experiments. On the basis of the partial structure factors, we investigated the origin of the first sharp diffraction peak. Disorder affects differently the localization properties of valence and conduction band states, as suggested by experimental mobilities of electrons and holes.

PACS numbers: 61.43.–j, 61.20.Ja, 71.25.Mg, 71.55.Jv

Liquid and amorphous forms of silicon dioxide are interesting because they constitute a prototypical example of a network-forming disordered material [1] and also in view of the general importance of SiO_2 for geophysics and for electronic industry applications. The atomic structure of the various forms of SiO_2 at low pressure is characterized by a very flexible but otherwise very stable tetrahedral atomic network which can persist up to high temperature in the liquid state.

The chemical bonds between Si and O combine ionic and covalent character and can easily adjust to different atomic environments. An accurate treatment of the electronic bonding is therefore essential to describe disordered forms of SiO_2. However, due to the complexity of the system, first-principles electronic structure calculations have only been performed so far for crystalline forms of SiO_2 [2–4]. Numerical studies of liquid (l-) and amorphous (a-) SiO_2 have been limited to empirical classical potentials [5,6], which do not explicitly contain information on the electronic structure.

In this Letter we report the results of an *ab initio* molecular dynamics (MD) simulation of l-SiO_2 at 3500 K, followed by a rapid quench to 300 K. In the liquid, broken bonds and coordination defects occur but the tetrahedral network remains rather stable even at 3500 K. Interestingly, in spite of the limited relaxation allowed by our fast cooling rate, we recovered a tetrahedral network with perfect short range order by quenching from the melt. Our quenched structure is in good agreement with neutron diffraction data for a-SiO_2 [7,8]. Our calculated partial structure factors give insight on the origin of the first sharp diffraction peak (FSDP) in the neutron structure factor, which is an issue that has attracted considerable interest [6,9–11]. The electronic density of states (DOS) of our amorphous model agrees with x-ray photoemission (XPS) data. Finally, the effect of disorder and temperature on the band gap and the carrier mobilities is correlated with the properties of the electronic wave functions.

We performed constant volume Car-Parrinello (CP) simulations [12]. The electronic structure was described within density functional theory in the local density approximation (LDA) [13]. We adopted a plane wave pseudopotential (PP) approach using a conventional PP [14] for silicon and an ultrasoft PP for oxygen [15]. The method is given in Ref. [16]. The ultrasoft PP requires only a small set of plane waves to describe the valence wave functions of oxygen. This allows us to model disordered forms of SiO_2 with a sufficiently large unit cell.

Good convergence in the ground-state electronic properties was achieved with cutoff of 16 Ry for the wave functions and of 150 Ry for the augmented electron density. In this way, the experimental Si-O bond length in molecules such as SiO_2 and SiO was reproduced within 1%. For the Si-O-Si bond angle in the molecule H_3Si-O-SiH_3, we obtained 146°, very close to experiment (144°) [17]. In addition, our calculation gave lattice constants and internal parameters of α-quartz within 2% of experiment, in accord with a recent LDA calculation [4].

We used a periodic cubic cell of side 10.45 Å containing 72 atoms to model l-SiO_2. The density (2.10 g/cm^3) was determined by extrapolating to $T = 3500$ K the data for the liquid of Ref. [18]. We started the simulation from a configuration generated by Monte Carlo using the empirical potential of Ref. [6]. We let the atomic coordinates and the electronic wave functions at the Γ point of the supercell evolve according to the CP equations of motion. The preconditioning scheme of Ref. [19] (with $\mu_0 = 400$ a.u. and $E_p = 3$ Ry) allowed us to increase the time step from 8 to 13 a.u. (0.31 fs). This was important to extend the time span of the simulation, in view of the low diffusion rates in l-SiO_2. A Nosé-Hoover thermostat [20] was used to keep the average ionic temperature of the simulation equal to a preset value T. At $T = 3500$ K, we found a closing of the band gap, and therefore we used a second thermostat on the electrons to keep the system on the Born-Oppenheimer surface [21].

 0031-9007/95/74(23)/4682(4)$06.00

We let the system evolve at temperatures ranging from 2500 to 3500 K for more than 6 ps. Then the temperature was fixed at 3500 K, well above the experimental melting point of $T_m = 2000$ K. Only at such a high temperature did we observe liquidlike diffusion. After 3 ps of equilibration, measurements were taken in the following 5 ps. At this point, each Si (O) atom had moved on average by more than 2 Å (2.7 Å) with respect to the initial configuration. Considering that the Si-O bond length is around 1.6 Å, this is a sufficiently long diffusion to lose memory of the initial configuration.

At $T = 3500$ K the mean squared displacement showed a strong correlation between oxygen and silicon motions. Our estimated diffusion constants are $(9 \pm 2) \times 10^{-6}$ cm^2/s for oxygen and $(5 \pm 1) \times 10^{-6}$ cm^2/s for silicon [22]. The ratio of the two constants is consistent with the mass ratio of the two elements. Strong dynamical correlations and small diffusivity values result from the persistence of a tetrahedral network. This is also indicated by the average coordination of silicon and oxygen atoms, which remained close to 4 and 2, respectively, all along the evolution. On average miscoordinated atoms occurred with a probability of less than 10%. These consisted of threefold and fivefold coordinated silicon and of onefold and threefold coordinated oxygen atoms.

In order to generate a model a-SiO_2, we first set the temperature of our system to 3000 K and took measurements for 3 ps. At this temperature, diffusion was already almost negligible on the time scale of the simulation. Then we quenched the system to 300 K in another 3 ps and finally we took measurements during the following 3 ps. In order to check the density of our generated amorphous structure, we studied its total energy as a function of the volume at $T = 0$ K. The resulting equilibrium density at zero external pressure was 2.14 g/cm^3, i.e., only 2% higher than the density that we chose for the simulation. This compares well with the experimental density of a-SiO_2 at standard pressure (2.20 g/cm^3), providing an *a posteriori* justification for our choice of the volume.

The average structures of liquid and amorphous samples determine the total neutron structure factors $S(q)$ which are displayed in Fig. 1. These have been obtained by weighting the calculated partial structure factors with the Si and O neutron scattering lengths [7]. In the case of a-SiO_2 the theoretical structure factor is compared with the $S(q)$ extracted from neutron diffraction experiments [7]. The agreement between theory and experiment is rather good over the entire range of q. The large amount of noise present in the theoretical data at low q, particularly in the amorphous case, is a consequence of our small simulation cell. Apart from thermal broadening at high temperature, the general features of the $S(q)$ of the liquid are similar to those of the amorphous, as one expects for a glass forming material. To our knowledge no experimental diffraction data for l-SiO_2 have been reported. Overall our total and partial structure factors are similar to those of recent classical MD calculations [6].

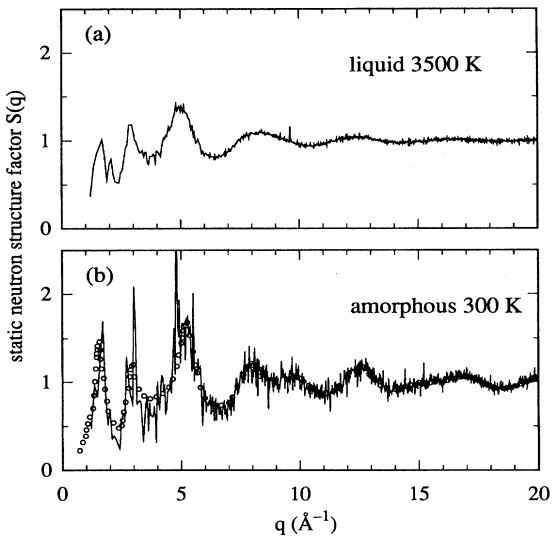

FIG. 1. Static neutron structure factor $S(q)$ for (a) liquid and (b) amorphous SiO_2. We have used the scattering lengths $b^{Si} = 4.149$ fm and $b^O = 5.803$ fm to calculate $S(q)$. Circles are experimental data from Ref. [7].

An important feature of the structure factors in Fig. 1 is the presence of a FSDP. It has been speculated that in both oxide and chalcogenide glasses this peak should arise from a peak in the concentration-concentration structure factor $S_{CC}(q)$ [23], mainly originating from Si-Si correlations [9]. This is at variance with the results of our simulation. In fact our calculated partial structure factors indicate that, in addition to Si-Si, O-O and Si-O correlations also contribute to the FSDP. Moreover, as can be seen in Fig. 2, we do not find a FSDP in our $S_{CC}(q)$. This is in agreement with the results of Ref. [6]. The situation appears to be different in liquid $GeSe_2$, for which recent experimental data show a prominent FSDP in $S_{CC}(q)$ [10]. This suggests that different mechanisms are at the origin of the FSDP in SiO_2 and in $GeSe_2$.

The simulated amorphous is characterized by the presence of a perfectly chemically ordered bond network in which Si-atom-centered tetrahedra are linked by corner-sharing O atoms. Although a few edge-sharing tetrahedra were found in the liquid at $T = 3500$ K, these configurations were absent in the amorphous sample. Real space structural data are summarized in Table I, showing good agreement between theory and experiment. A feature of our amorphous structure is the sharpness of O-Si-O bond angle distribution centered at the tetrahedral angle. The Si-O-Si bond angle distribution is much broader, extending from 110° to 180°. This appears to be the most prominent effect of disorder in a-SiO_2 and reflects the large flexibility of bridging oxygen configurations. The average Si-O-Si bond angle is ~136°, slightly smaller than in crystalline forms of SiO_2. This is also smaller than the most probable values inferred from x-ray diffraction measurements (144° [24]) or from NMR experiments (140°–150° [25]) in a-SiO_2.

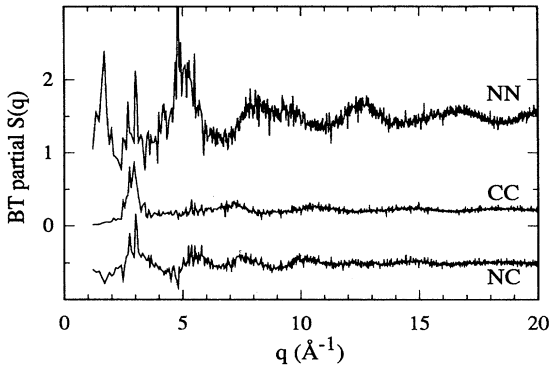

FIG. 2. The number-number (NN), concentration-concentration (CC), and number-concentration (NC) partial neutron structure factors for our model amorphous [23]. For clarity, the NN (NC) curve has been shifted up (down) by 0.5 (−0.5).

The calculated electronic DOS for l- and a-SiO_2 are reported in Fig. 3(a). We also show in Fig. 3(b) the DOS of α-quartz for comparison. The latter agrees well with other calculations; for instance, our band gap of 5.6 eV compares well with the value of 5.8 eV in Ref. [3]. As usual in LDA calculations, the experimental band gap (~9 eV [26]) is substantially underestimated. The strong similarity between the amorphous and the crystalline DOS is a consequence of the fact that the short range order is essentially the same in the two structures. Thus the states can be classified in a similar way in both structures; namely, the states at about −20 eV are oxygen 2s states, the states from −10 to −4 eV are bonding states between Si sp^3 hybrids and O (mainly) 2p orbitals, the highest occupied states above −4 eV are O 2p nonbonding orbitals, while the lowest conduction band states have antibonding character [3].

Experimentally the fundamental absorption edge of a-SiO_2 is found to be shifted to lower energies by ~0.5 eV with respect to α-quartz [27]. This trend is reproduced in our calculations where the shift is of ~0.8 eV. More subtle differences between α-quartz and a-SiO_2 appear in the occupied valence states as can be seen from the experimental XPS data [28] shown in Fig. 3. Interestingly, all the relevant experimental features are also found in the calculated DOS, providing further support for the accuracy of our model amorphous.

TABLE I. Structural properties of disordered SiO_2. Lengths and full widths at half maximum (FWHM) in Å, angles in degrees, $\bar{l}$ average bond length, and $\bar{\theta}$ average bond angle.

	Liquid (MD 3500 K)		Amorphous (MD 300 K)		Amorphous (experiment)
	$\bar{l}$	FWHM	$\bar{l}$	FWHM	l[a]
Si-O	1.67	0.27	1.62	0.08	1.610 ± 0.050
O-O	2.73	0.68	2.68	0.21	2.632 ± 0.089
Si-Si	3.07	0.52	2.98	0.25	3.080 ± 0.100
	$\bar{\theta}$		$\bar{\theta}$		θ[b]
O-Si-O	109 ± 16		109 ± 6		
Si-O-Si	134 ± 19		136 ± 14		140-150

[a]The peak bond length from neutron scattering Ref. [8].
[b]The most probable bond angle from NMR Ref. [25].

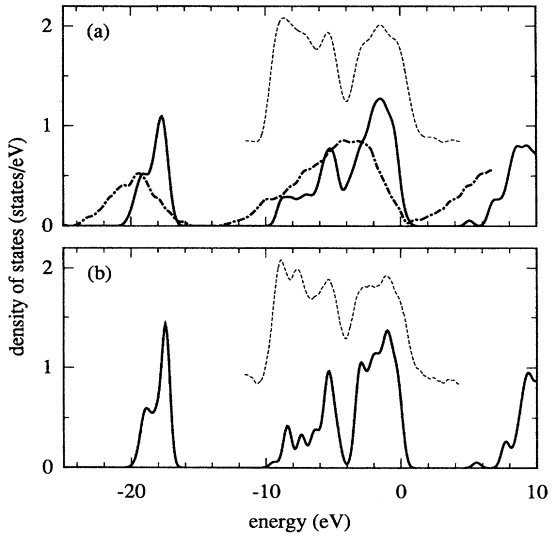

FIG. 3. Density of electronic states (DOS) of (a) amorphous SiO_2 at 300 K (solid) and (b) of α-quartz (solid). The insets (dashed) are XPS results from Ref. [28]. The dash-dotted curve in (a) is the DOS of the liquid at 3500 K. The theoretical curves are broadened with a Gaussian function of width $\sigma = 0.25$ eV and the highest occupied states are aligned at 0 eV.

The DOS of l-SiO_2 reported in Fig. 3(a) shows a large broadening of the bands which leads to a complete closing of the gap. Lowering the temperature to $T = 3000$ K gave rise to a gap of about 2 eV, suggesting a strong temperature dependence of the gap induced by disorder.

In order to investigate the effect of disorder on the localization properties of the electron states we have calculated the corresponding participation ratio [29]. This quantity, which is given in Fig. 4, measures the fraction of cell volume occupied by an eigenstate. Although the DOS of amorphous and crystalline SiO_2 are very similar, the participation ratio shows important differences in the two cases. In particular, the valence band states of a-SiO_2 are significantly more localized than those of crystalline SiO_2, whereas the conduction band states show similar localization properties in the two cases. This is consistent with the behavior found experimentally for electron and hole mobilities in a-SiO_2 [30]: electrons in a-SiO_2 do not show a localized character and behave similar to electrons in crystalline semiconductors; holes in a-SiO_2 show instead an activated behavior typical of localized states. We suggest that the difference in localization of valence and conduction band states in a-SiO_2 can be understood on the basis of the following qualitative argument. All the valence band states have an important weight on oxygen and are therefore affected by Si-O-Si bond angle disorder. This is true not only for O nonbonding states but also for bonding combinations between Si sp^3 and O p orbitals. In view of the large electronegativity difference between Si and O, the bonding orbitals have a large weight on oxygen atoms. The lowest conduction band states, instead, have

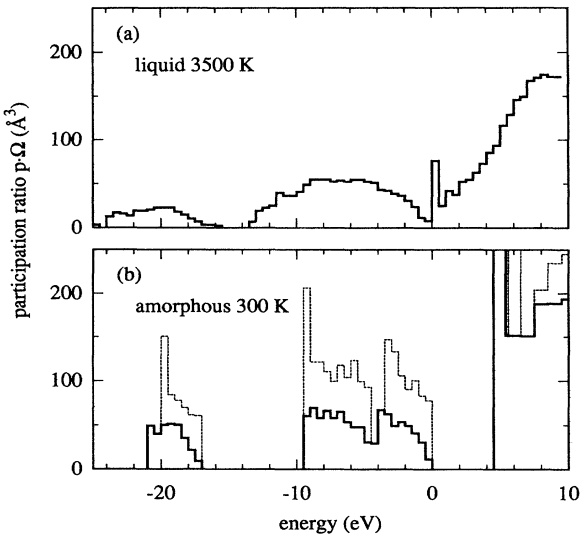

FIG. 4. Participation ratio $p \times \Omega$, the volume of the simulation cell, for (a) liquid and (b) amorphous SiO_2. Results for α-quartz (dashed) are reported in (b) for comparison.

antibonding character and a large weight on silicon atoms. The bond angle disorder on Si is very small as can be seen in Table I. Thus the effect of disorder on conduction band states is significantly smaller.

In the liquid at $T = 3500$ K the disorder is much larger both in Si-O-Si and in O-Si-O bond angles. Consequently the participation ratio reported in Fig. 4(a) shows localized character not only for the valence states but also for the unoccupied states that have filled the gap.

In conclusion, we have presented an *ab initio* MD study of disordered forms of SiO_2. In particular, the calculated partial structure factors of a-SiO_2 allowed us to characterize the microscopic origin of the FSDP. In our simulation, we compute electronic energies and wave functions in addition to the atomic trajectories. This allowed a comparison with the measured photoemission spectra and a realistic study of the effects of structural disorder on the electronic wave functions. This work can be considered as a first step for modeling defect processes in a-SiO_2.

We thank N. Binggeli and G. Galli for useful discussions. We acknowledge support by the Swiss National Science Foundation under Grant No. 20-39528.93. Calculations have been performed on the NEC-SX3 of the Swiss Center for Scientific Computing (CSCS) in Manno.

[1] *The Physics and Technology of Amorphous SiO_2,* edited by R. A. B. Devine (Plenum Press, New York, 1988).

[2] D. C. Allan and M. P. Teter, Phys. Rev. Lett. **59**, 1136 (1987); C. Lee and X. Gonze, Phys. Rev. Lett. **72**, 1686 (1994); X. Gonze, J. C. Charlier, D. C. Allan, and M. P. Teter, Phys. Rev. B **50**, 13 035 (1994); F. Liu, S. H. Garofalini, R. D. King-Smith, and D. Vanderbilt, Phys. Rev. Lett. **70**, 2750 (1993).

[3] N. Binggeli, N. Troullier, J. L. Martins, and J. R. Chelikowsky, Phys. Rev. B **44**, 4771 (1991).

[4] X. Gonze, D. C. Allan, and M. P. Teter, Phys. Rev. Lett. **68**, 3603 (1992).

[5] L. V. Woodcock, C. A. Angell, and P. Cheeseman, J. Chem. Phys. **65**, 1565 (1976); T. F. Soules, J. Chem. Phys. **71**, 4570 (1979); S. K. Mitra, M. Amini, D. Finchham, and R. W. Hockney, Philos. Mag. B **43**, 365 (1981); B. P. Feuston and S. H. Garofalini, J. Chem. Phys. **65**, 1565 (1988); J. D. Kubicki and A. C. Lasaga, Am. Mineral. **73**, 941 (1988).

[6] P. Vashishta, R. K. Kalia, J. P. Rino, and I. Ebbsjö, Phys. Rev. B **41**, 12 197 (1990).

[7] S. Susman *et al.,* Phys. Rev. B **43**, 1194 (1991).

[8] P. A. V. Johnson, A. C. Wright, and R. N. Sinclair, J. Non-Cryst. Solids **58**, 109 (1983).

[9] S. R. Elliot, Phys. Rev. Lett. **67**, 711 (1991).

[10] I. Penfold, P. Salmon, Phys. Rev. Lett. **67**, 97 (1991).

[11] M. Wilson and P. Madden, Phys. Rev. Lett. **72**, 3033 (1994).

[12] R. Car and M. Parrinello, Phys. Rev. Lett. **55**, 2471 (1985).

[13] We use the interpolation formulas given in J. P. Perdew and A. Zunger, Phys. Rev. B **23**, 5048 (1981).

[14] G. B. Bachelet, D. R. Hamann, andM. Schlüter, Phys. Rev. B **26**, 4199 (1982).

[15] D. Vanderbilt, Phys. Rev. B **41**, 7892 (1990).

[16] A. Pasquarello, K. Laasonen, R. Car, C. Lee, and D. Vanderbilt, Phys. Rev. Lett. **69**, 1982 (1992); K. Laasonen, A. Pasquarello, R. Car, C. Lee, and D. Vanderbilt, Phys. Rev. B **47**, 10 142 (1993).

[17] W. Airey, C. Glidewell, A. G. Robiette, and G. M. Sheldrick, J. Mol. Struct. **8**, 413 (1971).

[18] J. F. Bacon, A. A. Hasapis, and J. W. Wholley Phys. Chem. Glass **1**, 90 (1960).

[19] F. Tassone, F. Mauri, and R. Car, Phys. Rev. B **50**, 10 561 (1994).

[20] S. Nosé, Mol. Phys. **52**, 255 (1984); W. G. Hoover, Phys. Rev. A **31**, 1965 (1985).

[21] P. Blöchl and M. Parrinello, Phys. Rev. B **45**, 9413 (1992).

[22] The error bars have been determined by considering the fluctuations of the mean square displacement in our MD simulation. Because of the limited statistics, our error estimates should only be taken as indicative.

[23] A. Bhatia and D. Thornton, Phys. Rev. B **2**, 3004 (1970).

[24] R. Mozzi and B. Warren, J. Appl. Crystallogr. **2**, 164 (1969).

[25] R. Dupree and R. F. Pettifer, Nature (London) **308**, 523 (1991).

[26] F. J. Himpsel, Surf. Sci. **168**, 764 (1986); F. J. Grunthaner and P. J. Grunthaner, Mater. Sci. Rep. **1**, 65 (1986).

[27] A. Appleton, T. Chiranjivi, and M. Jafaripour, in *The Physics of SiO_2 and Its Interfaces,* edited by S. T. Pantelides (Pergamon Press, New York, 1978).

[28] B. Fischer, R. A. Pollak, T. H. DiStefano, and W. D. Grobman, Phys. Rev. B **15**, 3193 (1977); R. B. Laughlin, J. D. Joannopoulos, and D. J. Chadi, Phys. Rev. B **20**, 5228 (1979).

[29] D. J. Thouless, Phys. Rep. **13**, 93 (1974).

[30] N. F. Mott and E. A. Davis, *Electronic Processes in Non-Crystalline Materials* (Clarendon, Oxford, 1971).